Analysis of meteorological variables in the Australasian region using ground-and space-based GPS techniques

Yuriy Kuleshov, Suelynn Choy, Frank Fu, Fabrice Chane-Ming, Yuei-An Liou, Alexander G. Pavelyev

Analysis of Meteorological Variables in the Australasian Region Using Ground- and Space-based GPS Techniques

Yuriy Kuleshov[1,2,3,4,*], Suelynn Choy[2], Erjiang Frank Fu[1], Fabrice Chane-Ming[5], Yuei-An Liou[6] and Alexander G. Pavelyev[7]

[1] Bureau of Meteorology, Melbourne, Australia

[2] School of Mathematical and Geospatial Sciences, RMIT University, Melbourne, Australia

[3] Faculty of Sciences, Engineering and Technology, Swinburne University, Melbourne, Australia

[4] School of Mathematics and Statistics, The University of Melbourne, Melbourne, Australia

[5] Departmet Laboratoire de l'Atmosphère et des Cyclones, Université de la Réunion St Denis, Ile de la Réunion, France

[6] Center for Space and Remote Sensing Research (CSRSR), National Central University, Jhongli, Taiwan

[7] Kotelnikov Institute of Radio Engineering and Electronics of the Russian Academy of Sciences, Fryazino, Russian Federation

18 February 2016

* Corresponding Author: Professor Yuriy Kuleshov, Bureau of Meteorology, GPO Box 1289, Melbourne 3001, Australia

E-mail : y.kuleshov@bom.gov.au

Abstract

Results of analysis of meteorological variables (temperature and moisture) in the Australasian region using the Global Positioning System (GPS) radio occultation (RO) and GPS ground-based observations verified with *in-situ* radiosonde (RS) data are presented. The potential of using ground-based GPS observations for retrieving column integrated precipitable water vapour (PWV) over the Australian continent has been demonstrated using the Australian ground-based GPS reference stations network. Using data from the 15 ground-based GPS stations, state of the atmosphere over Victoria during a significant weather event, the March 2010 Melbourne storm has been investigated and it has been shown that the GPS observations has potential for monitoring the movement of a weather front that has sharp moisture contrast. Temperature and moisture variability in the atmosphere over various climatic regions (the Indian and the Pacific Oceans, the Antarctic and Australia) has been examined using satellite-based GPS RO and *in-situ* RS observations. Investigating recent atmospheric temperature trends over Antarctica, time series of the collocated GPS RO and RS data were examined and strong cooling in the lower stratosphere and warming through the troposphere over Antarctica has been identified, in agreement with outputs of climate models. With further expansion of the Global Navigation Satellite Systems (GNSS) system, it is expected that GNSS satellite- and ground-based measurements would be able to provide an order of magnitude larger amount of data which in turn could significantly advance weather forecasting services, climate monitoring and analysis in the Australasian region.

Key words: Temperature, Moisture, Remote sensing, Climate, Meteorology

1. Introduction

Conventional observations of meteorological variables (air pressure, temperature and moisture) are collected daily at thousands of meteorological stations around the world, to be used for weather analysis and forecasting. Subsequent statistical analysis of the archived data over long-term period (decades and longer) allows one to derive conclusions about climate (average state of weather) based on instrumental records obtained at meteorological stations. Conventional observations are well established and archives of meteorological variables recorded at many stations worldwide go back for more than a century. Such continuity of records is crucial for climate research, detection of historical trends in meteorological variables etc. However, conventional records are restricted to locations of meteorological stations.

In modern time, data obtained by optical, infrared, radio- and micro-wave remote sensing instruments revolutionised the science of meteorology and climatology as they provide potentially global coverage and consequently improved access to areas which have limited number of meteorological stations (data sparse areas) or not covered by conventional observations at all. Remote sensing data complement conventional observations and are widely used in numerical weather prediction, for climate monitoring and analysis adding value to and improving skill of weather forecasts, accuracy of trend analysis of meteorological variables etc. It is of particular importance for meteorological and climatological applications in the Southern Hemisphere where weather observation stations are much less in numbers than in the Northern Hemisphere. In this study, we present results of analysis of meteorological variables over data sparse areas using the measurements obtained by ground- and space-based techniques which utilise radio signals of the Global Positioning System (GPS).

Atmospheric water vapour is a critical component of the greenhouse effect and plays a significant role in the global climate system. The knowledge of the long-term spatial and temporal variability of water vapour is vital for understanding climate change. Ground-based GPS has long offered the prospect of complementing meteorological observations by providing integrated vertical column of precipitable water vapour (PWV) estimates beginning with pioneering studies of Bevis et al. (1992, 1994). There have been numerous studies since, over the USA, Japan, Korea, Europe, India, Taiwan and Antarctica which demonstrated usefulness of this methodology (Rocken et al., 1993; Seko et al., 2000, Liou et al., 2000a,b, 2001; Jade et al., 2005; Zhang et al., 2007; Bock and Nuret, 2009). One of the most valuable attributes of ground-based GPS-PWV is the ability to provide high temporal resolution and high accuracy of PWV estimates under all weather conditions at a very low cost. In this paper, we present results of deriving PWV using ground-based GPS reference stations network and investigate potential of the GPS-PWV methodology for monitoring of weather fronts.

Space-based instruments provide even wider (potentially global) coverage than regional ground-based networks, including the world ocean which covers about 70% of the Earth's surface. One of the emerging satellite remote sensing technique for obtaining atmospheric temperature and moisture records is GPS radio occultation (RO) methodology which provides all-weather capability, long-term measurement stability, high vertical resolution and high-accuracy measurements in the middle to upper troposphere, stratosphere and ionosphere (e.g. Rocken et al., 1997; Heise et al., 2006; Liou et al., 2007, 2010; Pavelyev et al., 2013; Kumar et al., 2014; Santi et al., 2014; Dhaka et al., 2015). High accuracy of the GPS RO methodology is of particular importance for reliable estimates of the atmospheric characteristics over the regions where conventional meteorological upper air observations from radiosondes (RS) are sparse or not available.

Evaluation of GPS RO methodology for retrieval of atmospheric profiles has been conducted in a number of studies in various regions (Wickert, 2004; Kuo et al., 2005; Fu et al. 2007; Rao et al., 2009) and high accuracy of retrieval of meteorological variables has been demonstrated. He et al. (2009) used GPS RO data to assess accuracy of temperature measurements by four types of RS in the upper troposphere and low stratosphere and demonstrated a close-to-zero mean difference between GPS RO and RS data for two types of radiosonds, Vaisala-RS92 and Shanghai radiosonde systems. However, large temperature biases are shown for the MRZ and VIZ-B2 radiosonde systems relative to GSP RO, which are probably caused by diurnal radiative effects (He et al., 2009).

This study is concerned with analysis of meteorological variables in the Australasian region (continent of Australia, Maritime continent, the Indian and the Pacific Oceans) and the Antarctic which are much less covered by meteorological observations than the Northern Hemisphere. Specifically, state of the atmosphere over the Australasian region and the Antarctic is investigated. The Australasian region is highly important in terms of impacts on weather and climate. The region is significant in meteorology because it is considered the most important energy source region in the entire global circulation system owing to a number of coincident factors, the most significant being geographical location and topography, both of which contribute to the development of the warmest large area of ocean on the Earth, the Tropical Warm Pool (Graham, 1994; Zhang et al., 1997). This is a region of intensive ocean-atmosphere interaction with widespread convection and environment favourable for tropical cyclone development. El Niño–Southern Oscillation (ENSO), a coupled ocean-atmosphere phenomenon in the central Pacific (Trenberth, 1997), is another significant climate driver of the planet which causes extreme weather (such as floods and droughts) in many regions of the world (Nicholls, 1993; Kuleshov et al., 2014). The Indian Ocean Dipole (IOD), a phenomenon which is similar to the ENSO in the Pacific, involves an

aperiodic oscillation of sea-surface temperatures and atmospheric pressure in the Indian Ocean (Saji et al., 1999) and its positive phase is associated with droughts in adjacent land areas of Indonesia and Australia. Consequently, accurate knowledge about state of the atmosphere over the Indian and the Pacific Oceans are vital for understanding the ENSO and the IOD and their impacts on climate of the Australasian and other regions of the planet. Here we present analysis of collocated GPS RO and *in situ* RS data over the Indian and the Pacific Oceans to demonstrate accuracy of GPS RO retrieval of atmospheric temperature and moisture profiles in the tropics.

The climate of Antarctica is the coldest on the Earth, with the lowest near-surface temperature of −89.2°C recorded at Vostok Station (Budretsky, 1984). However, due to a global warming, near-surface and air temperatures in Antarctica are rapidly increasing. Positive trend in near-surface temperature is well documented and significant warming of the Antarctic Peninsula was observed (King, 1994; Vaughan et al., 2001). Assessment of Antarctic near-surface temperature change has shown that significant warming extends well beyond the Antarctic Peninsula to cover most of West Antarctica. West Antarctic warming exceeds 0.1°C per decade over the past 50 years, and is strongest in winter and spring (Steig et al., 2009). Although this is partly offset by autumn cooling in East Antarctica, the continent-wide average near-surface temperature trend is positive. Analysing a complete temperature record for Byrd Station, a linear increase in annual temperature between 1958 and 2010 by 2.4±1.2°C has been found, establishing central West Antarctica as one of the fastest-warming regions globally (Bromwich et al., 2012). In fact, significant warming extends well beyond the Antarctic Peninsula and covers most of West Antarctica (Steig et al., 2009). However, there is no agreement on magnitude of atmospheric temperature trends over the Antarctic. Thus, reliable satellite remote sensing data are crucial for accurate estimation of atmospheric temperature variability over the vast areas of the Antarctic.

148 The total precipitation in Antarctica, averaged over the entire continent, is about 166
149 mm per year (Vaughan et al., 1999). According to the Köppen climate classification, areas
150 that receive less than 250 mm of precipitation per year are classified as deserts. As such, the
151 continent of Antarctica is largely a desert, apart from coastal areas with higher rate of
152 precipitation. Thus, the air over Antarctica is generally very dry and potential accuracy of air
153 temperature estimates as derived from GPS RO observations is high as the retrieval algorithm
154 depends on amount of moisture content (Rocken et al., 1997; Kuo et al., 2004). Here we
155 present analysis of vertical distribution of atmospheric temperature over polar region
156 (Antarctica) derived from GPS RO observations, to give another example of value of remote
157 sensing data for providing essential upper air data in the Southern Hemisphere where RS
158 network is extremely sparse.
159
160 **2. Data and Methods**
161 To analyse the state of the atmosphere over the Australasian region, we used GPS RO
162 data from FORMOSAT-3/COSMIC (F3C) mission. F3C is the first GPS RO mission that
163 employs a satellite constellation for RO observations and the constellation consists of six Low
164 Earth Orbit satellites (Liou et al., 2007; Fong et al., 2008a,b, Wickert et al. 2009). F3C was
165 launched in 2006 and the constellation is currently operational providing a large number of
166 daily observations. GPS RO data from F3C constellation were obtained from COSMIC web
167 site http://www.cosmic.ucar.edu/. We analysed GPS RO temperature and moisture profiles
168 obtained by F3C constellation over the Australasian region. Six meteorological stations
169 located in the tropics and having high quality of RS records have been selected for
170 comparison (Fig. 1, the selected stations are highlighted by green circles). Five years of RS
171 data (2006-2010) have been compared with GPS RO collocated events. In this study, GPS
172 RO collocated profiles have been selected to satisfy criteria of (i) spatial collocation to be

within 300 km radius from geographic position of the meteorological site, and (ii) temporal collocation to be less than 3 hours before or after the time of RS launch (spatial and temporal collocation criteria have been defined based on results of Zhang et al., 2011). Number of atmospheric profiles for RS and GPS RO events at the selected tropical sites is presented in Table 1.

Tropical air over the Australian region is generally warm and moist; however, there is a distinct seasonality. In the Southern Hemisphere, November to April is a wet season and May to October is a dry season; this is translated into significant difference in distribution of rainfall, atmospheric moisture and temperature (for detail, see Zillman, 2001; Kuleshov, 2004). In terms of seasonal rainfall, climate of Australian tropics is classified as summer dominant, with marked wet summer and dry winter (Fig. 2). In this classification, the differences between summer and winter rainfall (Figs. 3 and 4, respectively) are used to identify six major climate zones. In Fig. 2, the median annual rainfall and seasonal incidence (the ratio of the median rainfall over the period November to April to the period May to October) is used to identify these six major zones across Australia. As evident from Figs. 3 and 4, in the tropics most of the rainfall occurs in the summer months and it is associated with the monsoon. Based on this classification, we stratified the observations between wet seasons, which also corresponds to tropical cyclone (TC) seasons (November to April) and dry, non-TC seasons (May to October).

To evaluate vertical distribution of atmospheric temperature over the Antarctic, we used GPS RO data obtained from the CHAllenging Minisatellite Payload for geoscientific research (CHAMP) mission (Wickert et al., 2001). CHAMP was launched in 2000 and for a decade the mission has been operational. As long records are essential to estimate climate change accurately, CHAMP data were selected to derive temperature trends over Antarctica. We use CHAMP data processed by UCAR (Level 2 wetPrf data from May 2001 to August

198 2008 available online at http://www.cosmic.ucar.edu/). CHAMP GPS RO data were analysed
199 at nine pressure levels (850, 700, 600, 500, 300, 200, 150, 100 and 50 hPa) and compared
200 with RS data obtained at seven Antarctic meteorological stations.

201 To investigate the potential of using ground-based GPS observations for retrieving
202 vertical column integrated PWV over the Australian continent, we utilised the data from the
203 Australian GPS reference stations network, e.g., the State of Victoria GPSnet (Department of
204 Environment and Primary Industries, 2013). The GPS-based methodology can be used for
205 retrieving column integrated PWV profiles from the time-varying tropospheric zenith path
206 delay, which can be retrieved by stochastic filtering of the GPS measurements (Bevis et al.
207 1992). In this study, the GPS-PWV estimates were derived using the GPS meteorology
208 method originally proposed by Bevis et al., 1992, 1994. GPS signals are delayed when
209 propagating through the troposphere and this delay is known as the Zenith Path Delay (ZPD)
210 or Zenith Total Delay (ZTD). The conversion from ZTD to PWV involves a two-step process.
211 The ZTD is divided into a hydrostatic term (known as Zenith Hydrostatic Delay, ZHD)
212 caused primarily by the dry gases in the atmosphere, and a wet term (known as Zenith Wet
213 Delay, ZWD) which is mainly contributed by water vapour contained in the atmosphere
214 (Davis et al., 1985). ZHD can be calculated given the local surface pressure and known
215 location of the GPS receiver. Subtracting ZHD from ZTD yields ZWD, from which PWV can
216 be estimated given near-surface air temperature. In our study, the ground-based GPS derived
217 PWV are integrated vertical column water vapour.

218 To validate remote sensing data obtained by F3C and CHAMP space missions and the
219 Australian GPS reference stations network, we used conventional upper air observations
220 obtained by RS. For meteorological stations located on the Australian continent, the RS data
221 were obtained from archive of the National Climate Centre, the Australian Bureau of
222 Meteorology. In Fig. 1, location of observation stations of the Australian Upper Air Network

223 is presented. For the stations in Antarctica, RS records (monthly time series) were extracted
224 from the HadAT2 dataset of the Hadley Centre, UK Met Office (Thorne et al., 2005),
225 available online at http://hadobs.metoffice.com/hadat/hadat2.html.

226 RS are the primary operational source of upper air observations including pressure,
227 temperature and moisture; for this reason they are used for independent validation of GPS-
228 PWV and GPS RO data. A RS flight ascends to 2 km in 7–8 minutes, and reaches 5 km in
229 about 20 minutes after the launch. As the temporal variability of the GPS-PWV and GPS RO
230 in these time scales is not significant GPS-derived values are often taken at times when RS
231 flights are released (e.g. 11:00 UTC and 23:00 UTC). It is these values of RS data that were
232 used for comparison with GPS-PWV and GPS RO data using the collocation criteria
233 described above.

234 While coastal areas of Australia are reasonably covered by the RS network,
235 geographic distribution of the stations in the interior of the continent is very sparse. Similarly,
236 vast areas of the Indian Ocean, the Pacific Ocean and the Antarctic are covered by only a few
237 stations. On the other hand, satellite-based measurements provide global coverage and
238 thousands of atmospheric pressure, temperature and moisture profiles could be obtained daily
239 over remote areas with limited conventional observations. For example, F3C provides
240 approximately 2,500 daily GPS RO events globally. This is a comparable amount of
241 atmospheric profiles to those obtained by the global RS network which has about 2,000
242 stations worldwide. On average, the Australasian region obtains around 300 RO events daily
243 (Fig. 1) which is more than a number of atmospheric profiles that 38 Australian RS stations
244 provide. Similarly, ground-based Australian GPS/GNSS reference stations network provides
245 observations of much higher density (and frequency) than the upper air stations network (RS
246 are typically launched only once or twice a day). For example, there are 15 GPSnet stations in
247 Victoria within a 200 km radius from central Melbourne and only one RS station. Thus,

248 remote sensing methodologies which provide high accuracy of retrieval of meteorological
249 variables have great potential not only to complement conventional observations but in the
250 near future to become a superior source of data for meteorology and climate research and
251 applications.

252 In the next section, we present results of the GPS ground- and space-based
253 atmospheric moisture and temperature retrievals validated with *in situ* RS data to demonstrate
254 value of these remote sensing methodologies for detailed description of vertical structure of
255 the atmosphere in various climatic regions (from the tropics to polar areas), potential for
256 enhancing severe weather forecasting and deriving accurate estimates of atmospheric
257 temperature trends.

258

259 **3. Results**

260 ***3.1. Atmospheric moisture retrieval over the Australian continent from GPS ground-based***
261 ***and RS data***

262 We verified accuracy of GPS-PWV data using RS data at two sites of the Australian
263 Bureau of Meteorology Upper Air Network. The selected meteorological stations were
264 Melbourne Airport in Victoria and Wagga Wagga in New South Wales located within close
265 proximity to the GPSnet stations - Melbourne Observatory (MOBS) and Wagga Wagga
266 (WGGA). The separation distance is 22 km between MOBS and Melbourne Airport RS site
267 and 10 km between WGGA and Wagga Wagga RS site. As for height difference, it is 78 m
268 between Melbourne Airport and MOBS and 11 m between WGGA and Wagga Wagga.
269 Comparing one-week of GPS-PWV and RS-PWV estimates at these stations, good agreement
270 between the GPS and RS PWV data has been found, with the uncertainties in the GPS-PWV
271 of the order of 2–3 mm. This level of uncertainty agrees with previous studies (Tregoning et
272 al., 1998; Liou 200a,b, 2001, Feng et al., 2001, 2003; Wang et al., 2007; Thomas et al., 2011),

273 demonstrating that GPS can be used with confidence as a supplementary sensor for
274 atmospheric water vapour to complement observations from the Bureau's upper air network .
275 Here we present a case study to investigate potential applicability of the GPS-PWV
276 methodology for weather forecasting, specifically for monitoring of weather fronts. In this
277 study, 15 ground-based GPS stations from the Victorian GPS infrastructure network, i.e.
278 GPSnet, were used (refer to Fig. 5) to examine if the GPS observations could be used to
279 monitor the movement of weather fronts prior to severe thunderstorm occurrences. The March
280 2010 Melbourne storm, which brought heavy rainfall, large hail stones, strong winds and
281 flash flooding to the state of Victoria was selected as a case study.
282 The March 2010 Melbourne storms were a series of storms that passed directly over
283 Greater Melbourne. In the days before the storm, a large mass of warm, humid air had passed
284 down from the state of Queensland, where it had caused record flooding in southern
285 Queensland. This warm air mass clashed with a cold and dry air of low pressure system
286 coming from the west generating severe thunderstorms. The first storm was generated in the
287 west of Victoria in the morning on 6 March. The storm cells then extended in a southeast
288 direction across the state between 14:00 to 17:00 AEDT (Australian Eastern Daylight time,
289 which is UTC +11:00 daylight saving), passing central Melbourne at around 14:40 AEDT. At
290 the storm peak on 6 March, a 400 km band of rain and hail stretched across the state moving
291 in a southeasterly direction.
292 Fig. 6 shows the GPS-PWV time series at the six GPSnet stations (their locations are
293 highlighted by yellow circles in Fig. 5) over the one-week period, i.e., a few days prior to and
294 after the storm passage. The PWV values range between 15 mm to 50 mm, with some distinct
295 variability caused by severe weather processes. It appears that the time series of PWV at all
296 stations are consistent. The fluctuations in the PWV time series can in fact be linked to the
297 variations in water vapour content in the troposphere, which coincide with the passing of the

298 storm cells. The PWV increases from around 20 mm to 40 mm on DOY 063 to 064 (4 to 5
299 March 2010), corresponding to the arrival of warm and moist pre-frontal air. The warm pre-
300 frontal air holds more water vapour than the cold post-frontal air mass. Thus as the warm pre-
301 frontal air passed through Greater Melbourne from west to east, the water vapour content in
302 the atmosphere increased steadily; and when the cold and dry post-frontal air moves through,
303 the amount of water vapour decreased from around 40 mm back to 20 mm.

304 Fig. 7 depicts a closer snapshot of the GPS-PWV time series at six selected GPSnet
305 stations in the western and eastern regions of Melbourne (a buffer radius of 200 km from
306 Melbourne CBD) on DOY 064 (5 March 2010). As the cold front moves eastward, the first
307 station to register a large drop in PWV was BALL, followed by APOL, BACC, MOBS,
308 ELLI, and YALL. This phenomenon occurred at slightly different times as seen in the time
309 series presented in Fig. 7. This shows that ground-based GPS stations located in different
310 parts of the state can remotely sense the passage of frontal air mass. This information could be
311 utilised to monitor and predict the course/direction of the frontal air. Furthermore, the ground-
312 based GPS technique is capable of providing continuous observations of the storm passage
313 with high temporal resolution. If the lateral distance between stations is known, then the
314 velocity of the frontal air passage can be estimated. The spatial distribution of the water
315 vapour content at two-hour intervals during the cold frontal air passage is shown in Fig. 8
316 (direction of the front is shown by an arrow on the top left panel). It illustrates the movement
317 of the cold dry post-frontal air mass as it passed eastward through Greater Melbourne. We
318 estimated the velocity of the frontal air passage from the ground-based GPS observations and
319 radar images and found that both estimates correspond well, providing the value of
320 approximately 35 km/hr.
321

3.2. Atmospheric temperature and moisture retrieval over the Australasian region and Antarctica estimated from GPS RO and RS data

Comparison of atmospheric temperature and moisture profiles obtained by RS and GPS RO over the Australasian region has been made over five year period from May 2006 to December 2010 at pressure levels from 1,000 hPa to 30 hPa. Data from six selected stations located in the South Indian and South Pacific Oceans (Table 1 and Fig. 1; location of the stations is highlighted by green circles) have been examined. The number of profiles was approximately evenly distributed between TC seasons (November to April) and non-TC seasons (May to October). In general, during TC seasons (Fig. 9a) good agreement between RS and GPS RO temperature profiles (differences < ±0.5°C) has been found at all stations for pressure levels from 400 to 50 hPa (at altitudes from about 6.5 km in the upper troposphere up to 25 km in the lower stratosphere, especially between 10-15 km). For pressure levels above 400 hPa (below 6.5 km altitudes), discrepancies ranging from 0.8 to 1.35°C were observed mainly due to high level of moisture in the lower troposphere which affects accuracy of algorithms for GPS RO temperature retrieval (see Rocken et al., 1997 and Kuo et al., 2004 for detail). It should be noted that the distance between RS and GPS RO profiles as well as types of RS instruments could also be important contributors to these differences (He et al., 2009). Similar, for non-TC seasons (Fig. 9b), good agreement between RS and GPS RO atmospheric temperature profiles (<±0.5°C) was observed at most pressure levels. Comparing to TC-seasons, the differences were reduced at pressure levels between 800 and 400 hPa, which we attribute to improving in accuracy of temperature retrieval due to lower atmospheric moisture in May-October compared to TC seasons. Large differences in RS-GPS RO temperature observations of about 1-1.3°C consistently observed at Tromelin may indicate an issue with RS data at this station; however, this investigation is out of scope for this study. Detailed comparison between daily GPS RO and RS data collocated in space

(latitudes<5°, longitudes<2.5°) also demonstrates that in general temperature differences are <2°C with minimum differences in the upper troposphere at altitudes between 10 and 15 km (see example for Gillot station (20.9°S 55.5°E) located in the South Indian Ocean during strong TC season 2007/2008 in Fig. 10).

In addition to temperature, atmospheric moisture profiles were also examined. Specific humidity was derived from vertical profiles of relative humidity and partial pressure of water vapour obtained by RS and GPS RO respectively. Differences in specific humidity for TC seasons (Fig. 11a) were <0.5 g/kg at Darwin, Townsville, Cocos Islands and Mahe for pressure levels below 850 hPa (at altitudes above 1.5 km) and at Antanarivo and Tromelin for pressure levels below 700 hPa (at altitudes above 2.5 km). Larger differences (from 1 to 2 g/kg for Darwin, Cocos Islands and Townsville) were observed at pressure levels above 900 hPa (at altitudes between the surface and about 1 km). Relative differences calculated as RS-GPS RO/GPS RO were <15-20% above 400 hPa (below 6.5 km) and < 30% below 350 hPa (above 7.5 km). Comparing atmospheric moisture profiles for TC seasons and non-TC seasons (Figs. 11a and 8b respectively) one can find that differences in values of specific humidity retrieved by RS and GPS RO were <0.5 g/kg for pressure levels below 700 hPa independently of the season with exception at Tromelin where the differences ranging from 0.5 to 1 g/kg were observed between 700 and 600 hPa pressure levels during TC period. Analysing moisture profiles, distinct difference in seasonal convective activity at Antanarivo, Darwin, Townsville and Tromelin was observed as the differences in specific humidity during non-TC and TC periods (see example for Darwin in Fig. 11c). High level of convective activity around Darwin during November to April (wet season or TC season) is well documented. On average, Darwin experiences more than 80 thunderstorms during the wet season which represents the highest thunderstorm activity in Australia (Kuleshov, 2012).

These findings are encouraging as they provide confidence that accuracy of GPS RO-derived temperature profiles in the tropics, despite high atmospheric moisture content, is comparable with that of RSs. Thus GPS RO data could be utilised effectively in tropical atmospheric wave studies in the upper troposphere and lower stratosphere during TC seasons in the Indian and the Pacific Oceans where RS data are available only from a few stations (Gubenko et al., 2008, 2011, Chane-Ming et al., 2014).

As for the Antarctic, six Antarctic coastal stations (Fig. 12) were selected after initial analysis of RS records based on the completeness of data records for the recent period (2000-2009) to validate the GPS RO temperature data. On average, less than 2-3% of RS data were missing at nine standard pressure levels from 850 to 50 hPa for these six stations. RS data from Amundsen-Scott station at the South Pole were also used to represent the interior areas of Antarctica, although the percentage of missing data was relatively high: 21 to 24% for the six standard pressure levels from 500 to 50 hPa. To enable the RS-RO comparison, GPS RO temperatures were sampled using a 500 km radius circles centred at each of the seven stations. The resulting GPS RO temperature series are referred to as the collocated RO temperature series hereafter, and are compared with the corresponding *in situ* RS temperature series.

It was found that at all seven stations and all nine pressure levels the collocated RO temperatures are generally in good agreement with the corresponding *in situ* RS temperatures, in terms of both the actual values and the seasonal cycle. In the lower stratosphere to the upper troposphere (from 50 hPa to 300 hPa), the collocated RO temperatures and their corresponding RS temperatures are in such good agreement that they are hardly distinguishable from each other (see example of RS (black) and GPS RO (blue) time series in Fig. 13). Similarly, very good agreement was found at other levels from 50 hPa to 300 hPa (not shown).

To investigate recent atmospheric temperature trends over the Antarctic, time series of the collocated RO and RS data were examined at each pressure level for the seven stations. Linear trends estimated from the collocated RO and RS temperature series are shown in Fig. 14. Strong lower-stratospheric cooling trends have been identified at all levels from 50 to 300 hPa for all Antarctic stations by both methods, with only two exceptions (at McMurdo (89664) RS data indicate positive trend at 50 hPa while GPS RO data indicate strong cooling, and at Novolazarevskaja (89512) RS data indicate negative temperature trend at 300 hPa while GPS RO data indicate a weak warming trend). The 7-station-mean stratospheric cooling rates at 200 and 100 hPa pressure levels are about -2.6°C and -3.2°C (or -2.1°C and -3.5°C) per decade from the collocated GPS RO (or RS) data, respectively (see the Means in Fig. 14). Once again, we note that both GPS RO and RS data are in excellent agreement for the low-stratospheric measurements at levels from 50 hPa to 300 hPa. In the troposphere (at levels below 300 hPa) both cooling and warming trends are detected at different stations depending on their geographical location; however, RO and RS data are less consistent in terms of detecting temperature trends in the lower to mid-troposphere than in the lower stratosphere. Nevertheless, for the stations in the Western Antarctica, Halley (89022) and Novolazarevskaja (89512), GPS RO data indicate warming trends in the upper troposphere at 500 hPa and 700 hPa pressure levels, in agreement with finding of earlier studies about rapid near-surface warming (Vaughan et al., 2001). For interior of Antarctica, cooling at all pressure levels from 50 to 500 hPa was found (Amundsen-Scott station, 89009).

4. Discussion

In this report on recent progress in advancing climate studies in the Australasian region we demonstrated that GPS satellite- and ground-based measurements are valuable source of meteorological data. We presented examples of distribution of atmospheric

420 characteristics over the Indian and the Pacific Oceans, continents of Australia and Antarctica
421 derived from GPS RO measurements and verified accuracy of RO temperature and moisture
422 retrieval with *in situ* RS data. Investigating recent atmospheric temperature trends over
423 Antarctica, time series of the collocated RO and RS data were examined and strong cooling in
424 the lower stratosphere and warming through the troposphere over the Antarctica has been
425 identified by both methodologies, with detected the strongest cooling trend of about -3°C per
426 decade at 100 hPa level. These findings demonstrate that GPS RO measurements could
427 significantly advance climate studies for data sparse areas like the Australasian region and the
428 Antarctic. Early study by Turner et al., 2006, through analysis of RS observations at nine
429 stations across Antarctica for the period 1971-2003 demonstrated cooling rates of about -
430 0.16°C per decade at 100 hPa. Our findings indicate that during 2001-2008 rate of cooling at
431 100 hPa level was much higher, about -3.2°C per decade. Our results are in agreement with
432 outputs of climate models which indicate that recent stratospheric cooling and tropospheric
433 warming are expected consequences of the observed increase in anthropogenic greenhouse
434 gas concentrations (IPCC AR5, 2013).

435 We also evaluated potential of the Australian network of GPS stations to estimate
436 moisture content of the atmosphere (PWV) and presented a case study for monitoring a severe
437 thunderstorm event using GPS-PWV methodology. Comparing GPS-PWV and RS-PWV
438 estimates at two selected stations in Victoria and NSW, good agreement between the GPS and
439 RS PWV data has been found, with uncertainties in the PWV estimates in the order of 2–3
440 mm, which is likely as radiosonde data are accurate to about 1.2 mm (e.g. Feng et al., 2003;
441 Wang and Zhang, 2008). Using data from the 15 ground-based GPS stations from the
442 Victorian GPS infrastructure network, we investigated state of the atmosphere over Victoria
443 during a significant weather event, the March 2010 Melbourne storm, and demonstrated that
444 the GPS observations has potential for monitoring the movement of a weather front that has

445 sharp moisture contrast. Using the ground-based GPS observations and weather radar images,
446 we estimated a velocity of the frontal air passage and found that both estimates correspond
447 well which demonstrates the potential of using GPS data for estimating the velocity of fronts.

448 These findings could have potentially important implications for enhancing reliability
449 and accuracy of severe weather forecasting services (Benevides et al., 2015; Shi et al., 2015;
450 Sparta and Rahman, 2016). Accurate estimates of time of front arrival at particular localities
451 are essential to provide early warning to public, aviation etc. about timing of expected
452 thunderstorm-related hazards (lightning, hail, strong winds and flash-flooding) associated
453 with passage of weather front. Lightning activity associated with thunderstorms in SE Asia
454 and Australia is high (Kar et al., 2009, Kuleshov et al., 2009, Liou and Kar, 2010) and it is
455 vital to accurately forecast time of thunderstorm development to provide general public with
456 early warning. This could potentially save lives (e.g., on average, 5 to 10 people are killed by
457 lightning in Australia annually (Lightning Protection, 2007) and significantly reduce
458 economic damage (e.g. the total damage attributed to Sydney storm in 1999, which was the
459 costliest natural disaster in Australian insurance history, was estimated around A$2.3 billion).
460 It is equally important for aviation weather forecasting, with implication for improving safely
461 of passengers and reduction of economic losses due to flights' delays or cancellations.

462 However, it should be noted, that not all fronts have such clear moisture signature as
463 the March 2010 Melbourne storm presented here as a case study. In general, GPS-PWV
464 methodology may be good for monitoring drylines as well as weather fronts with sharp
465 moisture contrast. There is another potential problem for monitoring weather fronts using
466 GPS-PWV which is related to measuring vertically integrated water column using this
467 technique rather than detecting near surface moisture feature of a front. This means that for a
468 strong front with less sharp moisture gradient, the frontal location may not be identifiable
469 from the GPS-PWV alone so accurately as it was demonstrated in section 3.1. Thus, in our

future research, we will address this issue of refining GPS-PWV methodology for application to severe weather forecasting utilizing additional surface-based and remote sensing data. A geographic information system (Chrisman, 2001) would be an invaluable tool for simultaneous analysis of multi-layered data sets of fields of atmospheric pressure and temperature, radar images, overlaid with GPS-PWV data and conventional meteorological observations to develop an operational system for weather front monitoring and enhancing severe weather forecasting services.

In this study, we extensively used F3C data. F3C, a constellation of six LEO satellites is one of the most successful missions which utilised GPS radio signals for meteorology and climate application. It is in operational use since 2006. Success of the F3C mission encouraged the development of the follow up mission - FORMOSAT-7/COSMIC-2 (F7C2) constellation of 12 LEO satellites. The first launch of six satellites of the low inclination constellation is planned for 2016 and the second launch of another six satellites into the high inclination orbits - for 2018. Consequently, significant increase in temporal and spatial coverage of the Australasian region by the RO events from F3C and F7C2 constellations with multiple Global Navigation Satellite Systems (GNSS) systems (i.e. GPS, GLONASS, Galileo and QZSS) is expected.

To summarise, in the near future, with further expansion of GNSS system, it is expected that GNSS satellite- and ground-based measurements would be able to provide much larger (an order of magnitude) amount of quality atmospheric data which in turn could significantly advance studies on climate analysis and monitoring in the Australasian region.

5. Concluding remarks

GPS RO technique has been recognized as an emerging technique for Earth's atmospheric observation. Atmospheric profiles derived from GPS RO observations provide

valuable information about state of the atmosphere over the oceans where upper air data from conventional meteorological observations are particularly scarce. With the recent GPS modernization and new global and regional GNSS systems in the near future, next generation RO missions will have opportunity and capability to utilise signals (in over ten different frequencies) from more than a hundred of GNSS satellites. As a consequence, the resolution, quantity and quality of the GNSS RO observations will be improved significantly and the data will have significant impact on various climatological and meteorological applications. Valuable information derived from GNSS RO atmospheric profiles would be utilised to improve accuracy of weather forecasting and climate studies. Similarly, data from GNSS ground-based stations (e.g. the Australian ground-based GPS/GNSS reference stations network) will provide accurate estimates of atmospheric moisture which could have positive impact on skill of weather forecasting and in longer terms assist with improving our understanding of the regional climate processes.

Acknowledgments: This work was partially supported by the RMIT Foundation and the Malcolm Moore Industry Research Grant and Taiwan NSC 102-2111-M-008-027 and NSC 102-2221-E-008-034 grants.

References

Benevides, P., Catalao, J., and Miranda, P. M. A., 2015: On the inclusion of GPS precipitable water vapour in the nowcasting of rainfall, *Nat. Hazards Earth Syst. Sci.*, **15**, 2605-2616, doi:10.5194/nhess-15-2605-2015.

Bevis, M, S. Businger, T. A. Herring, C. Rocken, R. A. Anthes, and R. H. Ware, 1992: GPS Meteorology: Remote Sensing of Atmospheric Water Vapor Using the Global Positioning System. *J. Geophy. Res.*, **99** (14), 787-801.

Bevis, M., S. Businger, S. Chiswell, T. A. Herring, R. A. Anthes, C. Rocken, and R. H. Ware, 1994: GPS Meteorology - Mapping Zenith Wet Delays onto Precipitable Water. *J. Appl. Meteorol.,* **33**, 379-386.

Bock, O., and M. Nuret, 2009: Verification of NWP Model Analyses and Radiosonde Humidity Data with GPS Precipitable Water Vapor Estimates during AMMA. *Weather Forecast.,* **24**, 1085-1101.

Bromwich, D.H., J.P. Nicolas, A.J. Monaghan, M.A. Lazzara, L.M. Keller, G.A. Weidner, and A.B. Wilson, 2012: Central West Antarctica among the most rapidly warming regions on Earth. *Nature Geoscience*, **6**(2), 139-145.

Budretsky, A.B., 1984: New absolute minimum of air temperatue. *Bull.Soviet Antarctic Expedition* (in Russian) (Leningrad: Gidrometeoizdat) 105.

Chane-Ming, F., C. Ibrahim, S. Jolivet, P. Keckhut, Y.-A. Liou, and Y. Kuleshov, 2014: Observation and a numerical study of gravity waves during tropical cyclone Ivan (2008). *Atmos. Chem. Phys.*, **14**, 641-658.

Chrisman, N.R., 2001: Exploring Geographic Information Systems. John Wiley. 270 pp.

542 Davis, J. L., T. A. Herring, I. I. Shapiro, A. E. E. Rogers, and G. Elgered, 1985: Geodesy by
543 Radio Interferometry: Effects of Atmospheric Modeling Errors on Estimates of
544 Baseline Length. *Radio Sci.,* **20**, 1593-1607.

545 Department of Environment and Primary Industries, 2013: Vicmap Position - GPSnet.
546 http://www.dse.vic.gov.au/property-titles-and-maps/maps-imagery-and-
547 data/data/gpsnet.

548 Dhaka, S. K., V. Kumar, R.K. Choudhary, Shu-Peng Ho, M. Takahashi, S. Yoden, 2015:
549 Indications of a strong dynamical coupling between the polar and tropical regions
550 during the sudden stratospheric warming event January 2009, based on
551 COSMIS/FORMOSAT-3 satellite temperature data, *Atmospheric Research,* **166**, 60-
552 69.

553 Feng, Y., Z. Bai, and A. Williams, 2001: GPS water vapour experimental results from
554 observations of the Australian Regional GPS Network (ARGN). In *2001 - A Spatial*
555 *Odyssey: 42nd Australian Surveyors Congress*, Brisbane, Australia.

556 Feng, Y., Z. Bai, P. Fang, and A. Williams, 2003: GPS water vapour experimental results
557 from observations of the Australian Regional GPS Network. *Geomatics Research*
558 *Australasia,* **79**, 21-41.

559 Fong, C.J., W.T. Shiau, C.T. Lin, T.C. Kuo, C.H. Chu, S.K. Yang, N. Yen, S.S. Chen, Y.H.
560 Kuo, Y.A. Liou, and S. Chi, 2008a: Constellation deployment for FORMOSAT-
561 3/COSMIC mission, *IEEE Trans. Geosci. Remote Sensing*, Vol. 46, No. 11, pp. 3367-
562 3379, doi:10.1109/TGRS.2008.2005202.

563 Fong, C.J., S.-K. Yang, C.-H. Chu, C.-Y. Huang, J.-J. Yeh, C.T. Lin, T.C. Kuo, T.-Y. Liu, N.
564 Yen, S.-S. Chen, Y.H. Kuo, Y.A. Liou, and S. Chi, 2008b: FORMOSAT-3/COSMIC
565 constellation spacecraft system performance: After one year in orbit, *IEEE Trans.*

566 *Geosci. Remote Sensing*, Vol. 46, No. 11, pp. 3380-3394, doi:
567 10.1109/TGRS.2008.2005203.

568 Fu, E., K., Zhang, F., Wu, X., Xu, K., Marion, A., Rea, et al., 2007: An evaluation of GNSS
569 radio occultation technology for Australian meteorology. *J. Global Positioning*
570 *Systems*, **6**, 74-79.

571 Graham, N. E., 1994: Decadal-scale climate variability in the tropical and North Pacific
572 during the 1970s and 1980s: observations and model results. *Clim. Dynam.*, **10**, 135–
573 162.

574 Gubenko, V.N., A. G. Pavelyev, and V. E. Andreev, 2008: Identification of wave origin of
575 temperature fluctuations and determination of the intrinsic frequency of internal gravity
576 waves in the Earth's stratosphere derived from radio occultation data. *J. Geophys. Res.*,
577 **113**, 1-9, D08109, doi:10.1029/2007JD008920.

578 Gubenko, V. N., A. G. Pavelyev, R. R. Salimzyanov, and A. A. Pavelyev, 2011:
579 Reconstruction of internal gravity wave parameters from radio occultation retrievals of
580 vertical temperature profiles in the Earth's atmosphere. *Atmos. Meas. Tech*. **10**, 2153–
581 2162, doi:10.5194/amt-4-2153-2011.

582 Heise, S., J. Wickert, G. Beyerle, T. Schmidt, and Ch. Reigberet, 2006: Global monitoring of
583 tropospheric water vapor with GPS radio occultation aboard CHAMP. *Advances in*
584 *Space Research*, **37**(12), 2222–2227.

585 He, W., S.-P. Ho, H. Chen, X. Zhou, D. Hunt, and Y.-H. Kuo, 2009: Assessment of
586 radiosonde temperature measurements in the upper troposphere and lower stratosphere
587 using COSMIC radio occultation data. *Geophys. Res. Lett.*, 36, L17807,
588 doi:10.1029/2009gl038712.

589 IPCC AR5, 2013: Working Group I Contribution to the IPCC Fifth Assessment Report
590 *Climate Change 2013: The Physical Science Basis.* Summary for
591 Policymakers,http://www.climate2013.org/images/uploads/WGI_AR5_SPM_brochure.
592 pdf.
593 Jade, S., M. S. M. Vijayan, V. K. Gaur, T. P. Prabhu, and S. C. Sahu, 2005: Estimates of
594 precipitable water vapour from GPS data over the Indian subcontinent, *J. Atmos. Sol-*
595 *Terr. Phy.,* **67**, 623-635.
596 Kar, S.K., Y.-A. Liou, and K.-J. Ha, 2009: Aerosol effects on the enhancement of cloud-to-
597 ground lightning over major urban areas of South Korea. *Atmospheric Research*,
598 Volume 92, No. 1, pp. 80-87, doi: 10.1016/j.atmosres.2008.09.004.
599 King, J. C., 1994: Recent climate variability in the vicinity of the Antarctic Peninsula. *Int. J.*
600 *Climatol.*, **14**, 357-369.
601 Kuleshov, Y. 2004. Seasonal and latitudinal variations of lightning ground flash activity in
602 Australia. *Aust. Met. Mag.* **53**, 197-204.
603 Kuleshov, Y., 2012: Thunderstorm and lightning climatology. Chapter 4, in book "*Modern*
604 *Climatology*", Intech, ISBN: 979-953-307-337-7, pp. 85-120.
605 Kuleshov, Y., D. Mackerras, and M. Darveniza, 2009: Spatial distribution and frequency of
606 thunderstorms and lightning in Australia. Chapter 8, in book "*Lightning: Principles,*
607 *Instruments and Applications".* Eds. H.D. Betz, U. Schuman, and P. Laroche, Springer,
608 189-209, doi 10.1007/978-1-4020-9079-0_8.
609 Kuleshov, Y., S. McGree, D. Jones, A. Charles, A. Cottrill, B. Prakash, T. Atalifo, S. Nihmei,
610 and F. L. S. K. Seuseu, 2014: Extreme weather and climate events and their impacts on
611 island countries in the Western Pacific: cyclones, floods and droughts**,** *Atmospheric*
612 *and Climate Science*, 4, 803-818. doi: 10.4236/acs.2014.45071.

613 Kumar, V., S.K. Dhaka, K.K. Reddy, A. Gupta, S.B. S. Prasad, V. Panwar, N. Singh, S-P Ho,
614 and M. Takahashi, 2014: Impact of quasi-biennial oscillation on the inter-annual
615 variability of the tropopause height and temperature in the tropics: A study using
616 COSMIC/FORMOSAT-3 observations, *Atmospheric Research,* **139**, 62-70.

617 Kuo, Y.-H., T. K. Wee, S. Sokolovskiy, C. Rocken, W. Schreiner, D. Hunt, and R. A. Anthes,
618 2004: Inversion and error estimation of GPS radio occultation data. *J. Meteor. Soc.*
619 *Japan,* 82B, 507–531.

620 Kuo, Y.-H., W. S. Schreiner, J. Wang, D. Rossiter, and Y. Zhang, 2005: Comparison of GPS
621 radio occultation soundings with radiosondes, *Geophys. Res. Lett.*, 32. L05817,
622 doi:10.1029/2004GL021443.

623 Lightning protection, 2007: Australian Standard / New Zealand Standard 1768:2007
624 (Prepared by the Standards Australia Committee EL-24), 199 p.

625 Liou, Y.-A., and C.-Y. Huang, 2000a: GPS observations of PW during the passage of a
626 typhoon. *Earth, Planets, and Space*, **52**(10), 709-712.

627 Liou, Y.-A., C.-Y. Huang, and Y.-T. Teng, 2000b: Precipitable water observed by ground-
628 based GPS receivers and microwave radiometry. *Earth, Planets, and Space*, **52**(6),
629 445-450.

630 Liou, Y.-A., Y.-T. Teng, T. Van Hove, and J. Liljegren, 2001: Comparison of precipitable
631 water observations in the near tropics by GPS, microwave radiometer, and radiosondes.
632 *J. Appl. Meteor*, **40**(1), 5-15.

633 Liou, Y.-A., A.G. Pavelyev, S. F. Liu, A.A. Pavelyev, N. Yen, C.Y. Huang, C. J. Fong, 2007:
634 FORMOSAT-3 GPS radio occultation mission: preliminary results. *IEEE Trans.*
635 *Geosci. Remote Sensing*, **45**(10), 3813-3826, doi:10.1109/TGRS.2007.903365.

636 Liou, Y.A., A.G. Pavelyev, S.S. Matugov, O.I. Yakovlev, and J. Wickert, 2010: Radio
637 occultation method for remote sensing of the atmosphere and ionosphere. ISBN 978-
638 953-7619-60-2, 176 p., I-Tech Education and Publishing KG, Croatia.
639 [http://www.intechopen.com/books/radio-occultation-method-for-remote-sensing-of-
640 the-atmosphere-and-ionosphere.]

641 Liou, Y.-A. and Kar, S.K., 2010: Study of cloud-to-ground lightning and precipitation and
642 their seasonal and geographical characteristics over Taiwan. *Atmospheric Research*,
643 95, 115–122, doi:10.1016/j.atmosres.2009.08.016.

644 Nicholls, N., 1993: ENSO, drought and flooding rain in Southeast Asia. pp 154-175 in:
645 South-east Asia's environmental future. The search for sustainability. Oxford Univ.
646 Press, 1993, 456 pp.

647 Pavelyev, A.G., K. Zhang, Y-A. Liou, A.A. Pavelyev, C.S. Wang, J. Wickert, T. Schmidt,
648 and Y. Kuleshov, 2013: Principle of locality and analysis of radio occultation data.
649 *IEEE Transactions on Geoscience and Remote Sensing,* **51**(6), 3240-3249,
650 doi:10.1109/TGRS.2012.2225629.

651 Rao, D. N., M. V. Ratnam, S. Mehta, D. Nath, S. G. Basha, V. V. M. J. Rao, B. V. K. Murthy,
652 T. Tsuda, and K. Nakamura, 2009: Validation of the COSMIC radio occultation data
653 over Gadanki: A tropical region. *Terr. Atmos. Ocean. Sci*., **20**, 50–70.

654 Rocken, C., R. H. Ware, T. Van Hove, F. Solheim, C. Alber, and J. Johnson, 1993: Sensing
655 Atmospheric Water Vapour wih the Global Positioning System. *Geophys.Res.Lett.,* **20**,
656 2631-2634.

657 Rocken C., R. Anthes, M. Exner, D. Hunt, S. Sokolovskiy, R. Ware, et al., 1997: Analysis
658 and validation of GPS/MET data in the neutral atmosphere. *J. Geophys. Res*., **102**,
659 29849-29866.

660 Saji N. H., B. N. Goswami, P. N. Vinayachandran, and T. Yamagata, 1999: A dipole mode in
661 the tropical Indian Ocean. *Nature*, 401, 360-363.
662 Santhi, Y. D., M. V. Ratnam, S.K. Dhaka, and S. V. Rao, 2014:
663 Global morphology of convection indices observed using COSMIC GPS RO satellite
664 measurements, *Atmospheric Research,* **137**, 205-215.
665 Seko, H., S. Shimada, H. Nakamura, and T. Kato, 2000: Three dimensional distribution of
666 water vapor estimated from tropospheric delay of GPS data in a mesoscale
667 precipitation system of the Baiu front. *Earth Planets Space,* **52**, 927-933.
668 Shi, J., Xu, C., Guo, J., Gao, Y., 2015: Real-Time GPS Precise Point Positioning-Based
669 Precipitable Water Vapor Estimation for Rainfall Monitoring and Forecasting, *IEEE*
670 *Transactions on Geoscience and Remote Sensing,* **53**(6), 3452-3459.
671 Sparta, W., and Rahman, R., 2016: Spatial interpolation of GPS PWV and meteorological
672 variables over the west coast of Peninsular Malaysia during 2013 Klang Valley Flash
673 Flood, *Atmospheric Research*, **168**, 205-219.
674 Steig, E., D. P. Schneider, S. D. Rutherford, M. E. Mann, J. C. Comiso, and D. T. Shindell,
675 2009: Warming of the Antarctic ice-sheet surface since the 1957 International
676 Geophysical Year. *Nature*, **457**, 459-462.
677 Thorne, P. W., D. E. Parker, S. F. B. Tett, P. D. Jones, M. Mc Carthy, H. Coleman and P.
678 Brohan, 2005: Revisiting radiosonde upper-air temperatures from 1958 to 2002, J.
679 Geophys. Res., 110, D18105, doi: 10.1029/2004JD005753.
680 Turner, J., T. A. Lachlan-Cope, S. Colwell, G. J. Marshall, and W. M. Connolley, 2006:
681 Significant warming of the Antarctic winter troposphere. *Science*, **311**, 1914-1917.

682 Thomas, I. D., M. A. King, P. J. Clarke, and N. T. Penna, 2011: Precipitable water vapor
683 estimates from homogeneously reprocessed GPS data: An intertechnique comparison
684 in Antarctica. *J. Geophys.Res.-Atmos.,* **116**, 2011.

685 Tregoning, P., R. Boers, D. O'Brien, and M. Hendy, 1998: Accuracy of absolute precipitable
686 water vapor estimates from GPS observations. *J. Geophys.Res.-Atmos.,* **103**, 28701-
687 28710.

688 Trenberth, K. E., 1997: The definition of El Niño *Bull. Amer. Met. Soc.*, **78**, 2771-2777.

689 Vaughan, D. G., J. L. Bamber, M. Giovinetto, J. Russell, and A. P. R. Cooper, 1999:
690 Reassessment of net surface mass balance in Antarctica. *J. Climate*, **12**, 933-945.

691 Vaughan, D. G., G. J. Marshall, W. M. Connolley, J. C. King, and R. Mulvaney, 2001:
692 Climate change: Devil in the detail. *Science*, **293**, 1777-1779,
693 doi:10.1126/science.1065116.

694 Wang, J. H., and L. Y. Zhang, 2008: Systematic errors in global radiosonde precipitable water
695 data from comparisons with ground-based GPS measurements. *J. Climate*, **21**, 2218-
696 2238.

697 Wang, J. H., L. Y. Zhang, A. Dai, T. Van Hove, and J. Van Baelen, 2007: A near-global, 2-
698 hourly data set of atmospheric precipitable water from ground-based GPS
699 measurements. *J. Geophys. Res.-Atm.,* **112**, D11107, doi:10.1029/2006JD007529.

700 Wickert, J., 2004: Comparison of vertical refractivity and temperature profiles from CHAMP
701 with radiosonde measurements. Danish Meteorological Institute, Scientific Report 04-
702 09. 27 p.

703 Wickert, J., Ch. Reigber, G. Beyerle, R. König, C. Marquardt, T. Schmidt, L. Grunwaldt, R.
704 Galas, T.K. Meehan, W.G. Melbourne, and K. Hocke, 2001: Atmosphere sounding by

GPS radio occultation: First results from CHAMP**,** *Geophys. Res. Lett.,* **28**(17), 3263-3266.

Wickert, J., T. Schmidt, G. Michalak, S. Heise, C. Arras, G. Beyerle, et al., 2009: GPS Radio Occultation with CHAMP, GRACE-A, SAC-C, TerraSAR-X, and FORMOSAT-3/COSMIC: Brief Review of Results from GFZ, in book 'New Horizons in Occultation Research', editors A. Steiner, B. Pirscher, U. Felsche, and G. Kirchengast. Springer-Verlag, Berlin Heidelberg. 3-15, doi:10.1007/978-3-642-00321-9.

Zhang, K., E. Fu, D. Silcock, Y. Wang, and Y. Kuleshov, 2011: An investigation of atmospheric temperature profiles in the Australian region using collocated GPS radio occultation and radiosonde data. *Atmospheric Measurent Techniques*, **4**, 2087–2092, doi:10.5194/amt-4-2087-2011.

Zhang, M., Y. Q., Ni, and F. Q. Zhang, 2007: Variational assimilation of GPS precipitable water vapor and hourly rainfall observations for a meso-beta scale heavy precipitation event during the 2002 Mei-Yu season. *Advances in Atmospheric Sciences,* **24**, 509-526.

Zhang, Y, J.M. Wallace, and D. S. Battisti, 1997: ENSO-like interdecadal variability: 1900–1993. *J. Climate,* **10**, 1004–1020.

Zillman, J. W., 2001, A hundred years of science and service, Bureau of Meteorology, Melbourne, 2001, 20 pp.

Table captions

Table 1. Geographical location of RS stations, number of RS and GPS RO atmospheric profiles and number of collocated profiles obtained from May 2006 to December 2010.

753 **List of Figures**

754 **Fig. 1.** Location of stations of the Australian Upper Air Network (red triangles) and a sample
755 of distribution of GPS RO events (black dots) over the Australasian region for one day.
756 Location of six RS stations in the tropics selected for comparison with GPS RO are
757 highlighted by green circles.

758 **Fig. 2.** Major seasonal rainfall zones of Australia.

759 **Fig. 3.** Average summer rainfall across Australia over the period 1961 to 1990.

760 **Fig. 4.** Average winter rainfall across Australia over the period 1961 to 1990.

761 **Fig.5**. Geographical location of the 15 selected GPSnet stations within 200 km radius from
762 Melbourne.

763 **Fig**. **6.** Time series of the seven days GPS-PWV (mm). Passage of the pre-, post-frontal air
764 and dissipation are marked on the time series. The different coloured lines represent the
765 different GPS stations marked in the figure on the right.

766 **Fig. 7.** A close-up snapshot of the GPS-PWV results from six GPS stations during the passage
767 of the weather front eastward through Greater Melbourne on DOY 64 (5 March 2010). The
768 different coloured lines represent the different GPS stations marked in the figure on the
769 left.

770 **Fig. 8.** Spatial distribution of water vapour content at two-hour interval during the weather
771 front passage within Greater Melbourne on DOY 64 (5 March 2010).

772 **Fig. 9.** Difference in temperature retrievals between collocated RS and GPS RO profiles for
773 six tropical stations (Antanarivo, Tromelin, Mahe, Cocos Island, Darwin and Townsville)
774 for May 2006 – December 2010 (a) during the Southern Hemisphere TC seasons
775 (November to April) and (b) non-TC seasons (May to October).

776 **Fig. 10.** Time-altitude distribution of atmospheric temperature at Gillot station, La Réunion
777 (20.9°S, 55.53°E) during strong tropical cyclone season in the south-west Indian Ocean

(2007-2008) derived from (a) daily GPS RO observations collocated in space (latitudes <5°, longitudes <2.5°) and (b) RS at 11:00UTC and (c) the difference.

Fig. 11. (a) and (b) same as in Figure 6 but for specific humidity. (c) Comparison of specific humidity derived from collocated RS (solid line) and GPS RO (dots) during the whole period of May 2006 to December 2010 (red), not-TC (green) and TC (blue) seasons for Darwin, Australia.

Fig. 12. Location of seven Antarctic stations used in this study to provide upper air data and 500 km radius circles centred at each station to encompass area of collocated GPS RO profiles.

Fig. 13. Comparison of atmospheric temperature time series, with trend lines superimposed, for *in situ* 100 hPa RS data (black) and the corresponding GPS RO data (blue) at the indicated stations.

Fig. 14. Comparison of linear trends of atmospheric temperature estimated from *in situ* RS data and the corresponding GPS RO data for the period from September 2001 to August 2008. Note that station 89009 (a high elevation station) has no RS data at 700 hPa and no bars are shown in the lower-right panel.

802 **Table 1.** Geographical location of RS stations, number of RS and GPS RO atmospheric
803 profiles and number of collocated profiles obtained from May 2006 to December 2010.

804

Radiosonde Station (latitude, longitude)	**Number of Profiles**	
	RS/ GPS RO profiles	***Collocated profiles***
Antananarivo (-18°48', 47°29')	2683 / 1616	700
Tromelin (-15°53', 52°11')	1306 / 1314	244
Mahe (-4°37', 55°27')	2390 / 785	306
Cocos Island (-12°30', 96°50')	1649 / 897	269
Darwin (-12°25', 130°50')	6730 / 983	949
Townsville (-19°15', 146°49')	5142 / 1546	1178

805

806

807

808

809

810

811

812

813

814

815

816

817

818

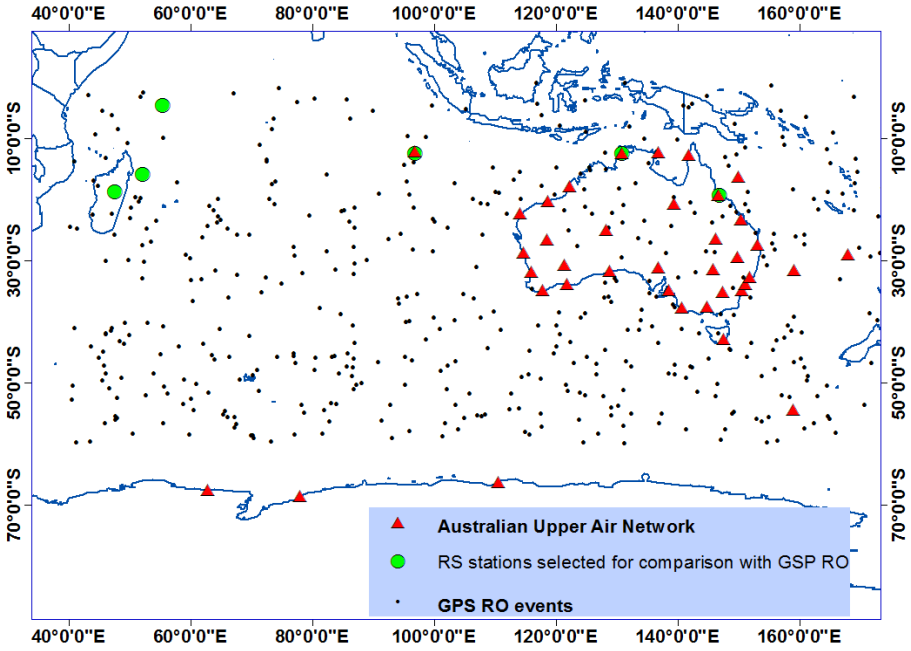

819

820 **Fig. 1.** Location of stations of the Australian Upper Air Network (red triangles) and a sample
821 of distribution of GPS RO events (black dots) over the Australasian region for one day.
822 Location of six RS stations in the tropics selected for comparison with GPS RO are
823 highlighted by green circles.
824

825

826 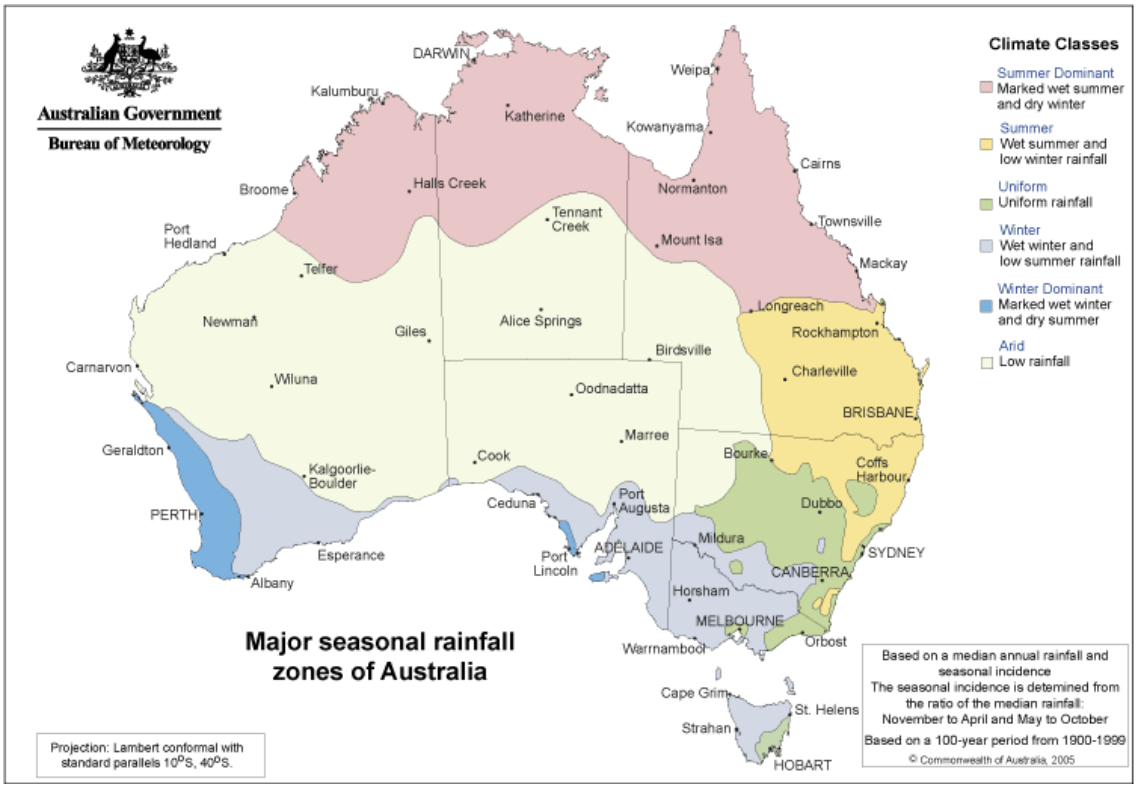

827

828 **Fig.2.** Major seasonal rainfall zones of Australia.

829

830

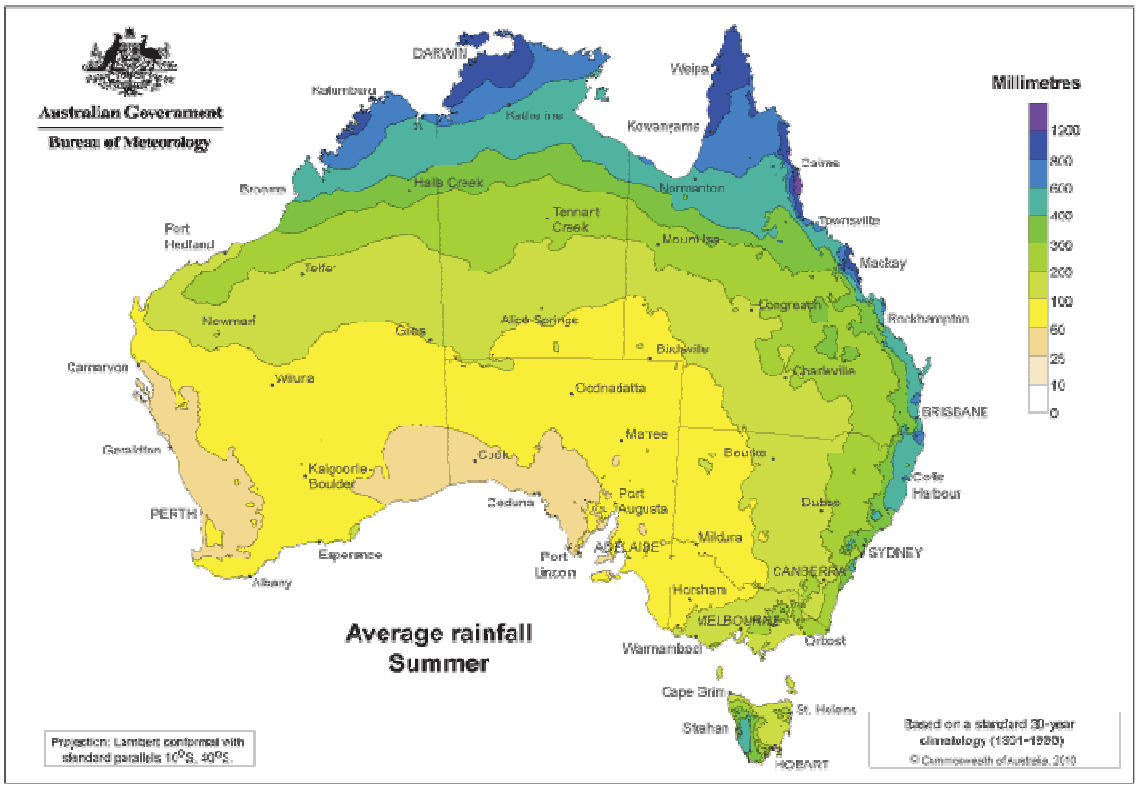

831

832

833 **Fig. 3.** Average summer rainfall across Australia over the period 1961 to 1990.

834

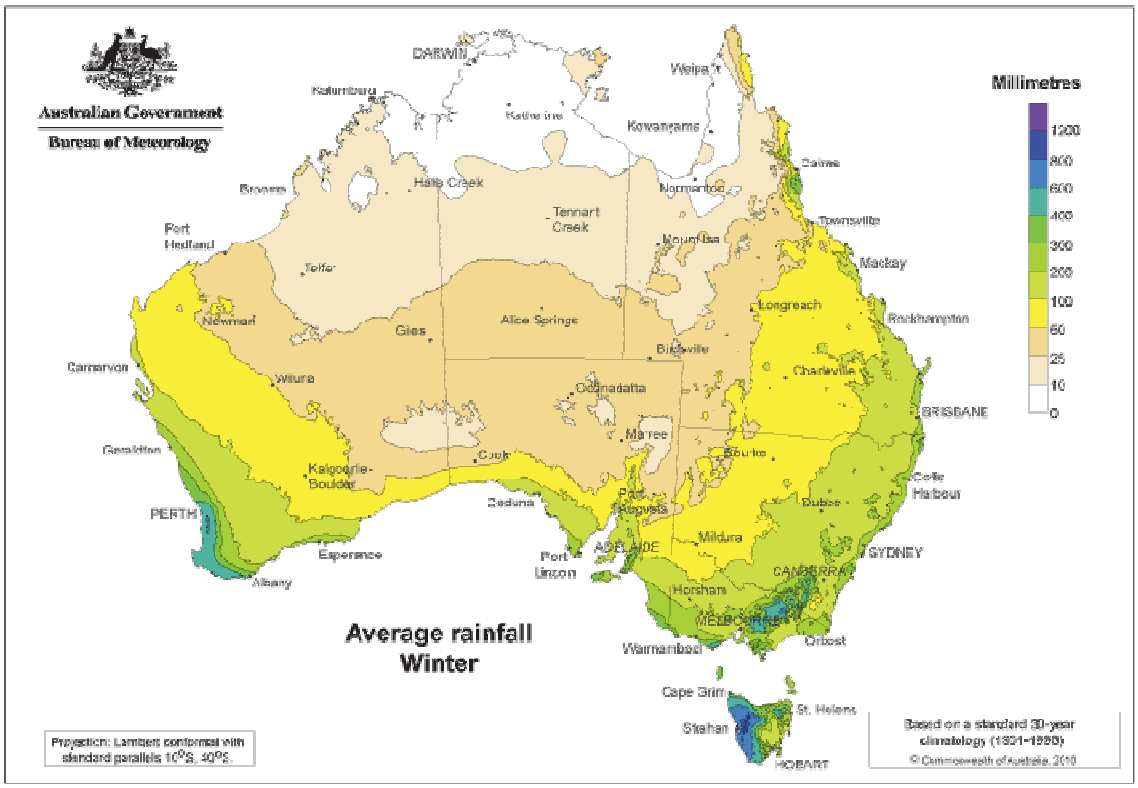

Fig. 4. Average winter rainfall across Australia over the period 1961 to 1990.

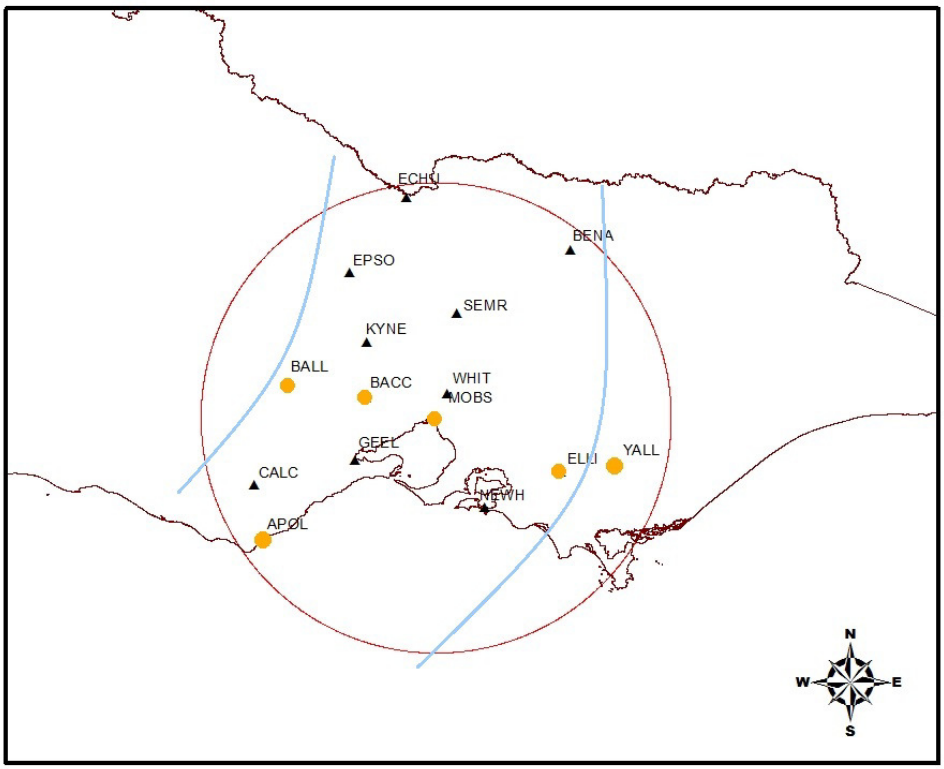

843

844 **Fig.5**. Geographical location of the 15 selected GPSnet stations within 200 km radius from
845 Melbourne with blue lines indicating locations of the front at 12 UTC (left) and 18 UTC
846 (right) (DOY 064, 5 March 2010), respectively.
847

848

849

850

851

852

853

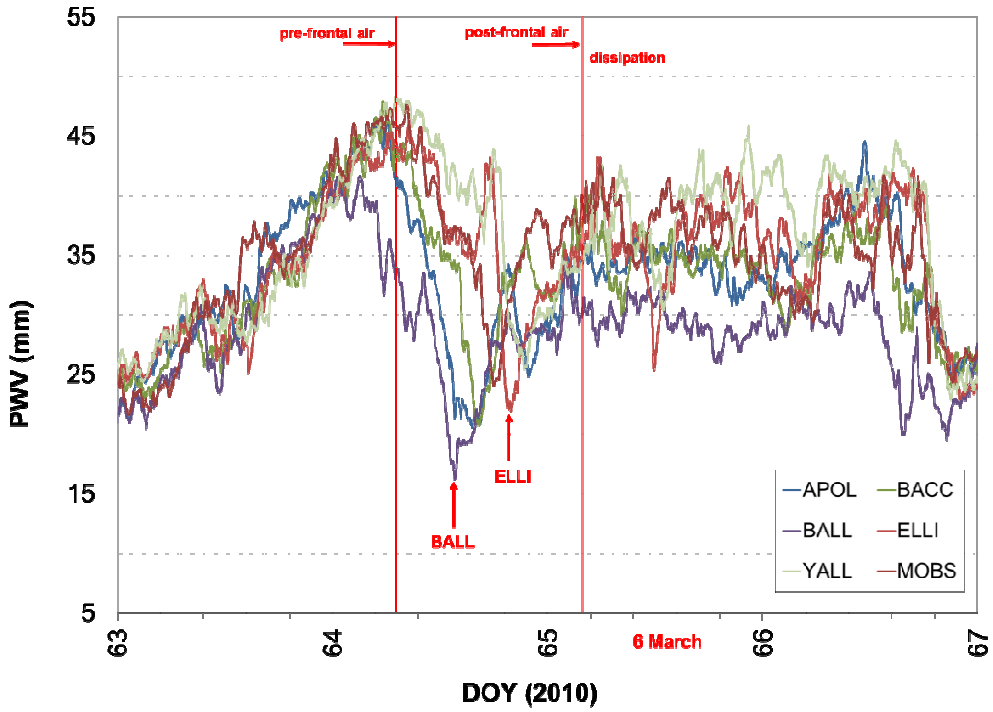

854

855 **Fig**. **6.** Time series of the seven days GPS-PWV (mm). Passage of the pre-, post-frontal air
856 and dissipation are marked on the time series. The different coloured lines represent the
857 different GPS stations marked in the figure on the right.
858
859

860

861

862

863

864

865

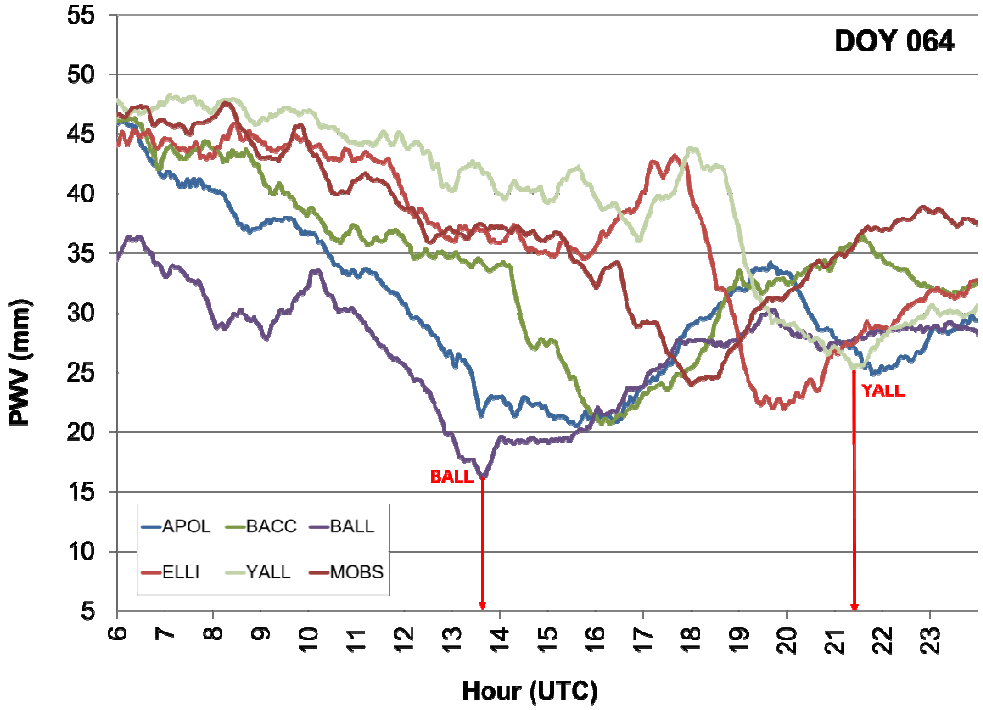

866

867 **Fig. 7.** A close-up snapshot of the GPS-PWV results from six GPS stations during the passage
868 of the weather front eastward through Greater Melbourne on DOY 64 (5 March 2010). The
869 different coloured lines represent the different GPS stations marked in the figure on the
870 left.
871

872

873

874

875

876

877

878

879

880

881

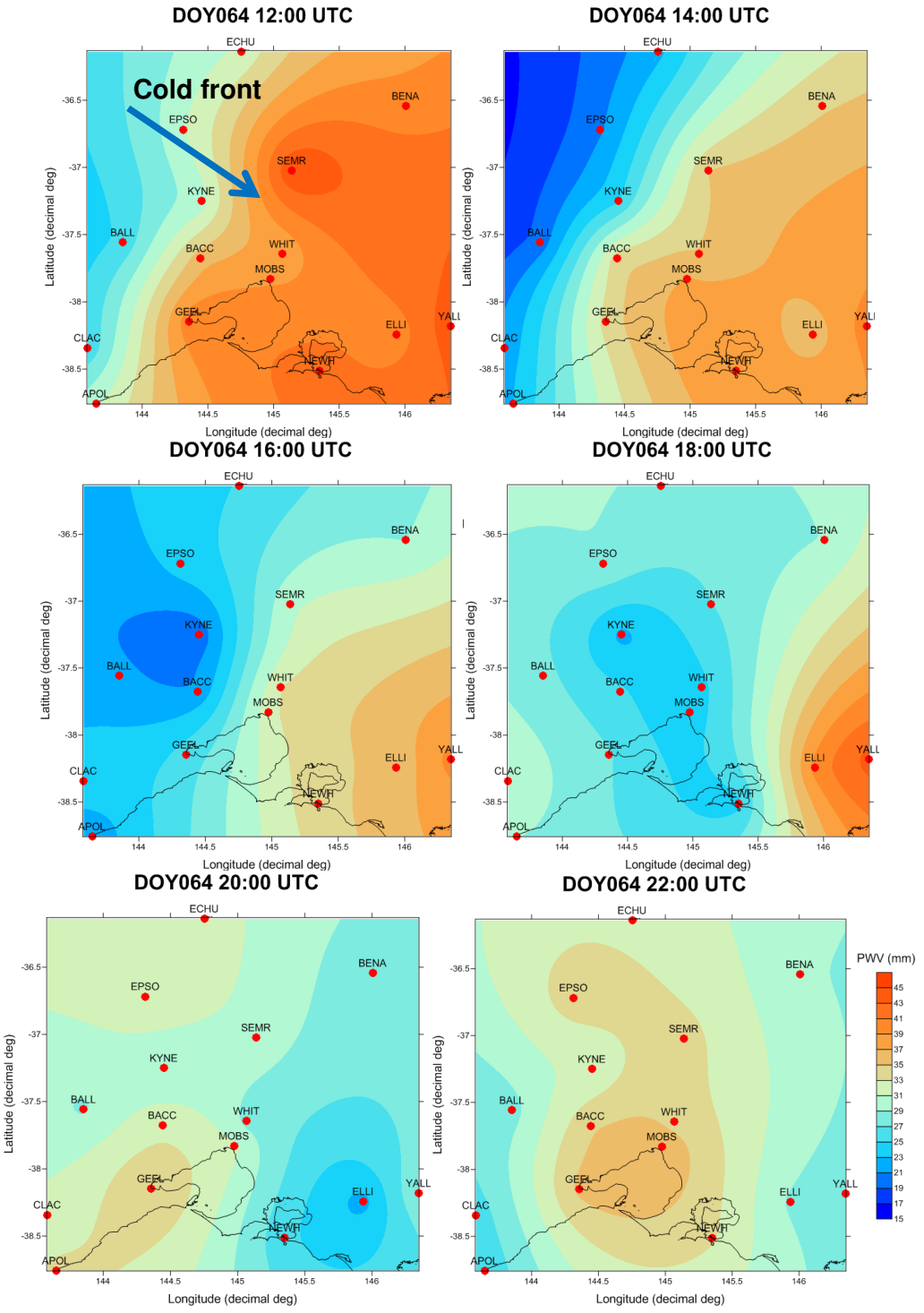

882 **Fig. 8.** Spatial distribution of water vapour content at two-hour interval during the weather
883 front passage within Greater Melbourne on DOY 64 (5 March 2010).
884

885

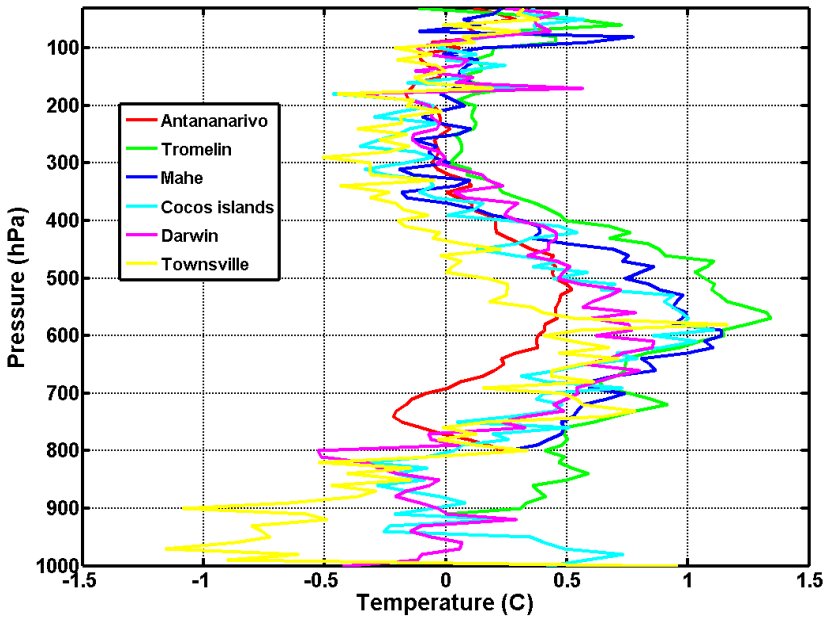

a)

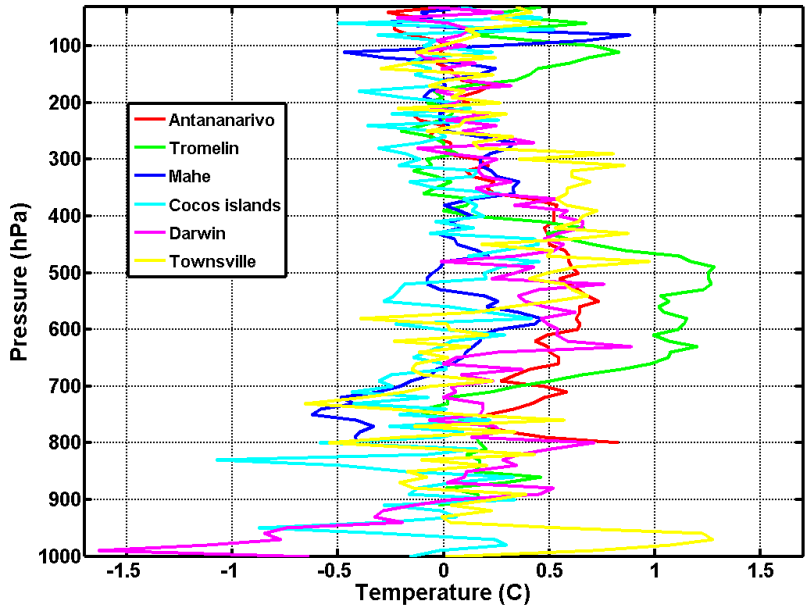

b)

Fig. 9. Difference in temperature retrievals between collocated RS and GPS RO profiles for six tropical stations (Antanarivo, Tromelin, Mahe, Cocos Island, Darwin and Townsville) for May 2006 – December 2010 (a) during the Southern Hemisphere TC seasons (November to April) and (b) non-TC seasons (May to October).

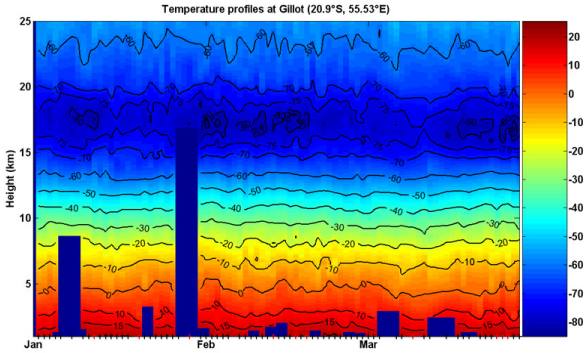

a)

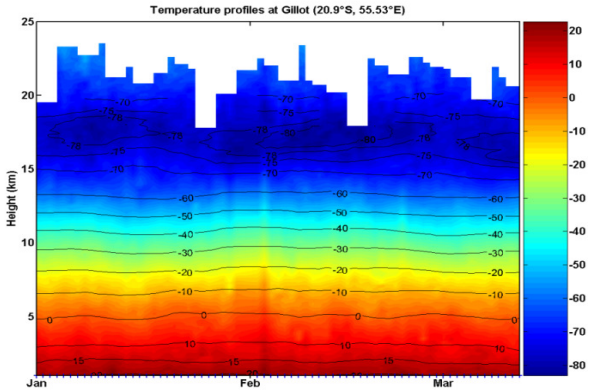

b)

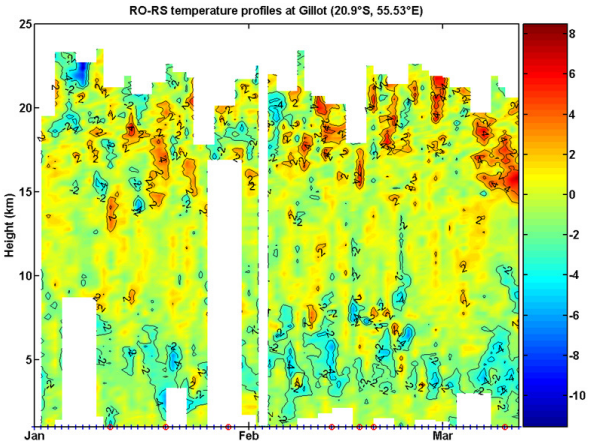

c)

Fig. 10. Time-altitude distribution of atmospheric temperature at Gillot station, La Réunion (20.9°S, 55.53°E) during strong tropical cyclone season in the south-west Indian Ocean (2007-2008) derived from (a) daily GPS RO observations collocated in space (latitudes <5°, longitudes <2.5°) and (b) RS at 11:00UTC and (c) the difference.

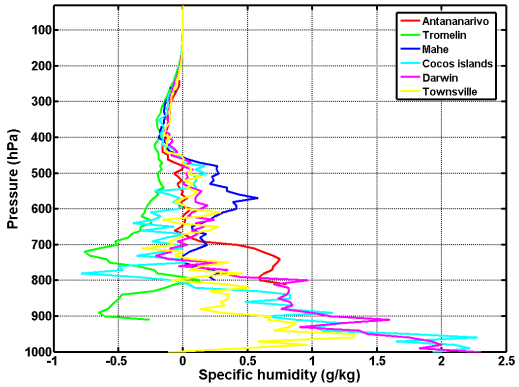

a)

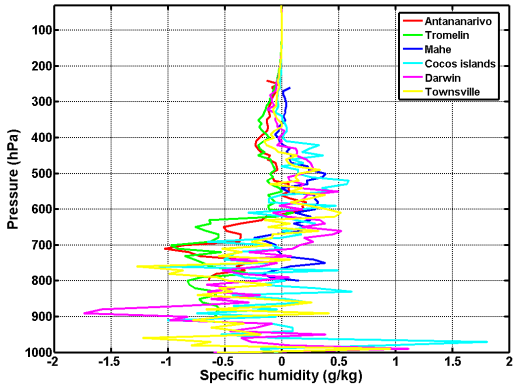

b)

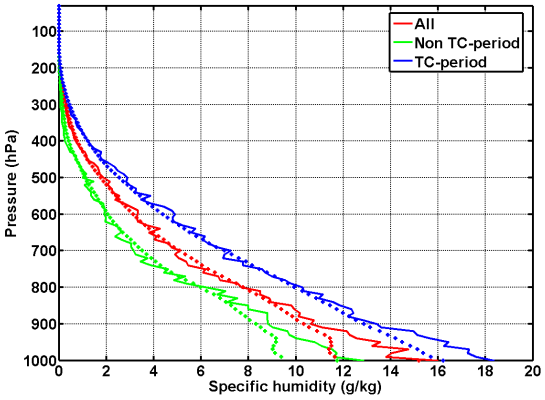

c)

905 **Fig. 11.** (a) and (b) same as in Figure 6 but for specific humidity. (c) Comparison of specific
906 humidity derived from collocated RS (solid line) and GPS RO (dots) during the whole
907 period of May 2006 to December 2010 (red), not-TC (green) and TC (blue) seasons for
908 Darwin, Australia.
909

910

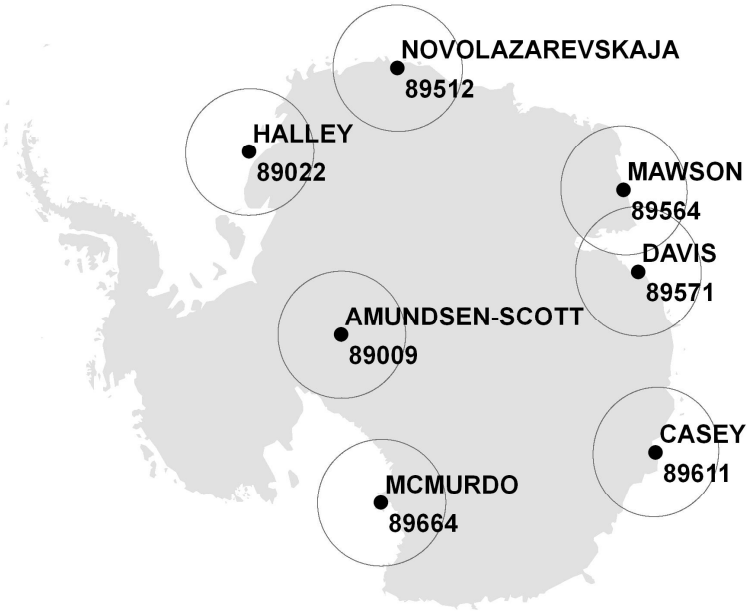

911

912 **Fig. 12.** Location of seven Antarctic stations used in this study to provide upper air data and
913 500 km radius circles centred at each station to encompass area of collocated GPS RO
914 profiles.
915

916

917

918

919

920

921

922

923

924

925

926

927

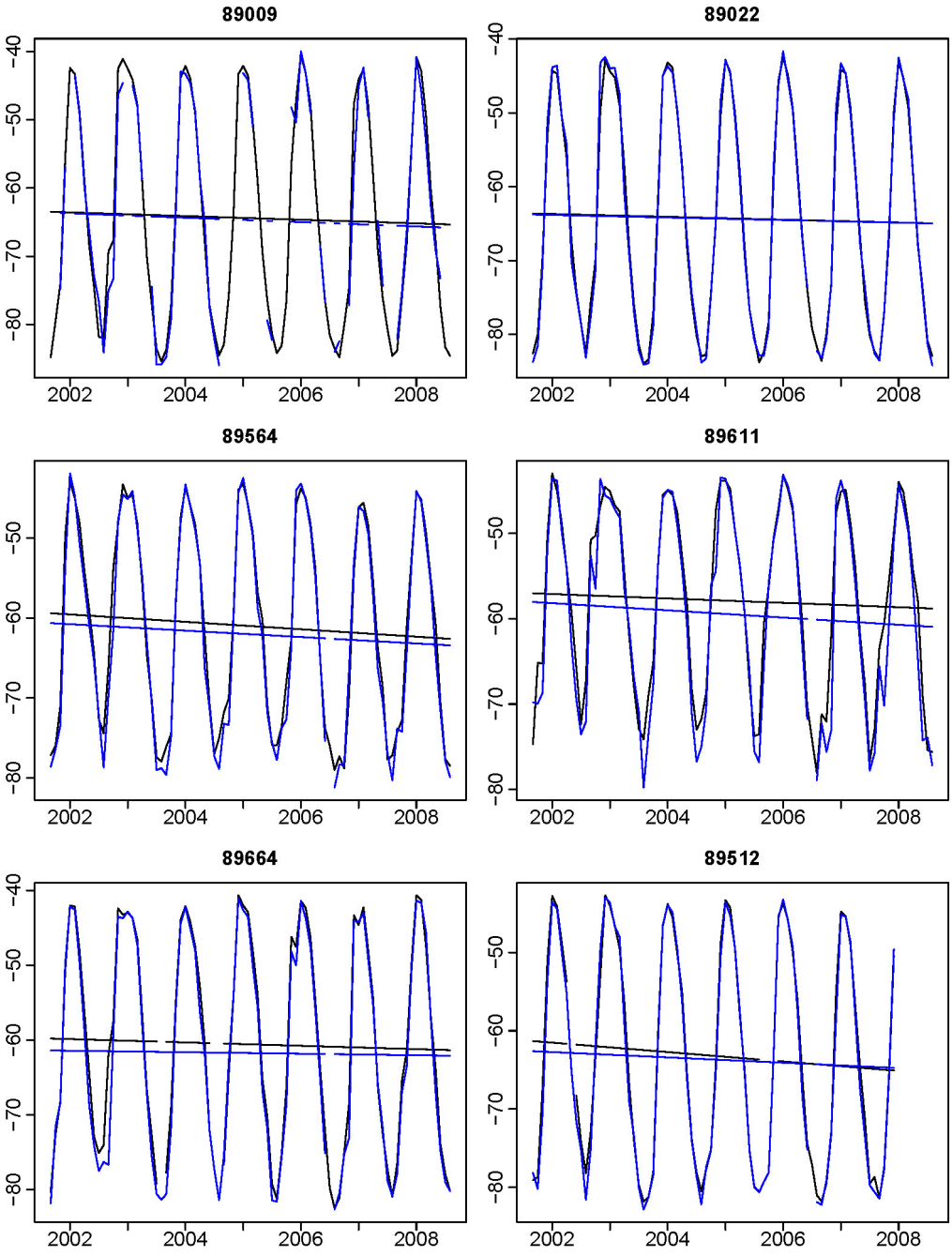

Fig. 13. Comparison of atmospheric temperature time series, with trend lines superimposed, for *in situ* 100 hPa RS data (black) and the corresponding GPS RO data (blue) at the indicated stations.

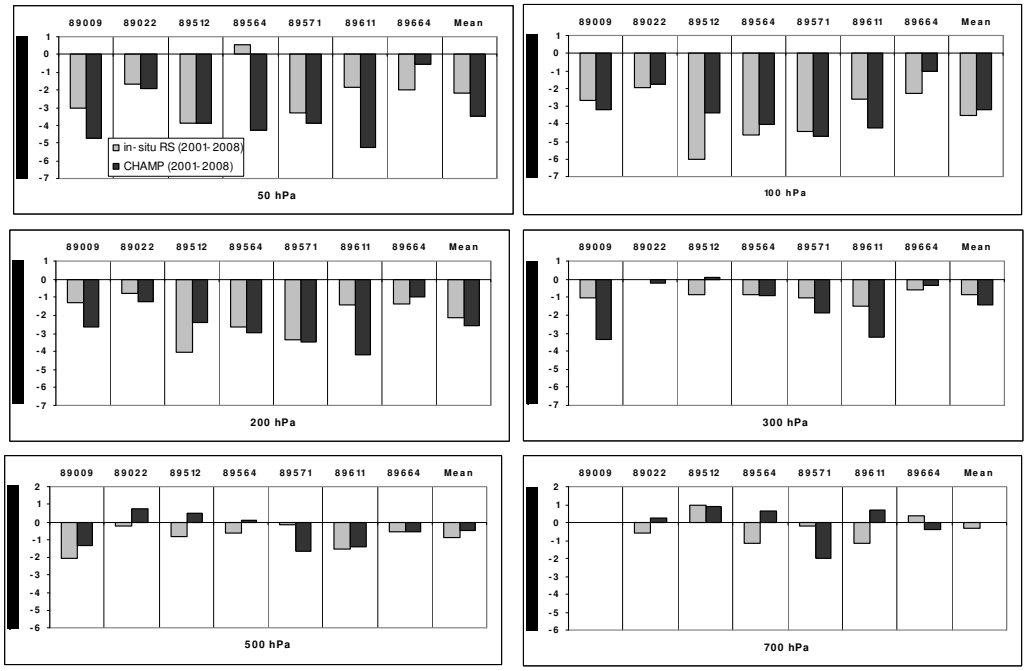

936

937 **Fig. 14.** Comparison of linear trends of atmospheric temperature estimated from *in situ* RS
938 data and the corresponding GPS RO data for the period from September 2001 to August
939 2008. Note that station 89009 (a high elevation station) has no RS data at 700 hPa and no
940 bars are shown in the lower-right panel.
941